Neuroimaging with [18F]THK-5351 PET in Progressive Supranuclear Palsy

著者	Ishiki A., Harada R., Tomita N., Watanuki S., Hiraoka K., Tashiro M., Kudo Y., Furukawa K., Okamura N., Arai H.
journal or publication title	CYRIC annual report
volume	2016-2017
page range	131-136
year	2017
URL	http://hdl.handle.net/10097/00128077

VII. 1. Neuroimaging with [^{18}F]THK-5351 PET in Progressive Supranuclear Palsy

Ishiki A.[1], Harada R.[2], Tomita N.[1], Watanuki S.[3], Hiraoka K.[3], Tashiro M.[3], Kudo Y.[4], Furukawa K.[5], Okamura N.[5], and Arai H.[1,4]

[1]Tohoku University Hospital
[2]Tohoku University Graduate School of Medicine
[3]Cyclotron and Radioisotope Center, Tohoku University
[4]Aging and Cancer, Tohoku University
[5]Tohoku Medical and Pharmaceutical University

Introduction

Tau positron emission tomography (PET) would be useful for the diagnosis of Alzheimer's disease (AD) and non-AD tauopathies, such as progressive supranuclear palsy (PSP), corticobasal degeneration (CBD), and some variants of frontotemporal lobar degeneration (FTLD). [^{18}F]THK-5351 was one of the first-generation tau PET radiotracers that was designed originally to detect tau aggregates in the form of PHF-tau in AD[1)]. Clinical PET studies in PSP and CBS patients have demonstrated prominent [^{18}F]THK-5351 retention in the midbrain and basal ganglia where tau pathology was observed frequently at autopsy[2,3)]. However, recent studies have suggested the existence of off-target binding to monoamine oxidase-B (MAO-B). Selegiline, a selective irreversible MAO-B inhibitor, substantially reduced [^{18}F]THK-5351 binding in the brain of patients with PSP as well as AD[4)]. In an autopsy case of AD, [^{18}F]THK-5351 PET signal reflects the combination of tau pathology and reactive astrocytes in the AD brain[5)]. However, what an [^{18}F]THK-5351 PET signal reflects in the PSP brain remains unclear. We examined imaging-pathology correlation in two autopsy-confirmed PSP patients who showed prominent tracer retention on an antemortem [^{18}F]THK-5351 PET scan.

Materials and methods

PET images were acquired using an Eminence STARGATE PET scanner. After intravenous injection of [^{18}F]THK-5351 (185 MBq) or [^{11}C]PiB (296 MBq), dynamic PET

images were obtained for 60 ([^{18}F]THK-5351) or 70 ([^{11}C]PiB) min. T1-weighted magnetic resonance images (MRI) were obtained using a SIGNA 1.5-Tesla machine. Standardized uptake value (SUV) images of [^{18}F]THK-5351 (40–60 min after injection) and [^{11}C]PiB (50–70 min after injection) were obtained. The regional SUV-to-cerebellar cortex SUV ratio (SUVR) was used as an index of tracer retention. SPM12 software and PMOD Ver. 3.7 software were used for image analysis.

The left hemisphere of the brain was immersed in 10% formalin for histology. The brain portions were frozen for biochemical analyses and unfixed tissue-based assays. Tissue sections of paraffin-embedded blocks were stained with Luixol fast blue and hematoxylin-eosin. Selected sections were stained with anti-tau AT8, anti-β-amyloid 4G8, anti-α-synuclein P-syn/81A, anti-TDP43 pS409/410–1, and anti-GFAP 6F2 antibodies.

Quantification of tau and glial fibrillary acidic protein (GFAP) immunoreactivity, in vitro autoradiography of [^{18}F]THK-5351 and [^{3}H]THK-5351, semiquantification of PHF-tau by immunoblotting, and quantification of MAO-B and GFAP by enzyme-linked immunosorbent assay (ELISA) were performed (previously reported[6]).

Results

Subject 1

An 84-year-old male presented with memory disturbance and disorientation. One year later, standing and gait became unstable with progression of extrapyramidal signs and PSP was diagnosed clinically. PET scans were performed 2 years after the diagnosis of PSP. At the time of the PET scan, he was bedridden and the Mini-Mental State Examination (MMSE) score was 1 of 30. The PSP rating scale score was 82. A brain MRI showed a typical "hummingbird sign". He died of aspiration pneumonia 295 days after the PET scan.

Subject 2

A 73-year-old male presented with memory disturbance. Mild cognitive impairment was diagnosed clinically 3 years after the first symptoms appeared. He gradually presented with speech impairment, stereotypical behavior, and change of food preference, and progressive nonfluent aphasia (PNFA) was diagnosed. One year later, he presented with unstable gait and was prone to falls. At the PET scan, he was bedridden and the MMSE score was 1 of 30. An MRI showed diffuse brain atrophy prominent in the right anterior temporal, hippocampus, amygdala, and caudate nuclei. He died of aspiration pneumonia 79 days after PET scan.

[^{18}F]THK-5351 and [^{11}C]PiB PET scans

Figure 1 shows the [^{18}F]THK-5351 PET images from the two subjects. Images from a cognitively normal individual are shown for comparison at the bottom. Subject 1 showed significant [^{18}F]THK-5351 retention in the globus pallidus and midbrain. Mild tracer retention was observed also in the other cortices, including parahippocampal and inferior temporal gyri. Subject 2 showed prominent [^{18}F]THK-5351 retention in the parahippocampal and inferior temporal gyri, as well as the globus pallidus and midbrain. No remarkable retention of [^{11}C]PiB was observed in the neocortex in both of the subjects.

Neuropathological examination

Brain weight in subject 1 was 1580 g. Autopsy revealed severe atrophy in the midbrain tegmetum, pons, subthalamic nucleus, and relatively mild atrophy in the frontal cortex, but not in the basal ganglia. Neuropathological examination revealed tau pathology in neuronal and glial cells consistent with PSP. Globose tangles were observed in the midbrain, pons, medulla, subthalamic nucleus, and nucleus basalis of Meynert. Moderate numbers of tufted astrocytes were observed also in the amygdala, motor cortex, and superior frontal gyrus. Neurofibrillary tangles were observed in the area which corresponded to age-related Braak stage II. The tau immunoreactivity density appeared greatest in the medial temporal regions, followed by the basal ganglia and frontal cortex. Gliosis and neuronal loss were observed also in the substantia nigra. However, amyloid-β, α-synuclein, and TDP-43 pathology were absent in this case.

Brain weight in subject 2 was 920 g. Autopsy revealed atrophy in the temporal lobes, midbrain, pons, globus pallidus, hypothalamic nucleus, and cerebellar dentate nucleus. There was neuronal loss in the pigmented neurons of the substantia nigra and locus coeruleus. AT8 immunostaining revealed abundant tau burden, including neurofibrillary tangles, globose tangles, tufted astrocytes, coiled bodies, and neuropil threads in the temporal, cingulate, frontal, striatum, globus pallidus, and subthalamic nucleus. In addition, thorn-shaped astrocytes, typical in aging-related tau astrogliopathy, were observed in the temporal lobe gray and white matter. Sparse amyloid plaques were observed. Both α-synuclein and TDP-43 pathology were absent in this case. Gliosis was severe in the bilateral hippocampus and amygdala. Astrocytosis with neuronal loss was prominent in the temporal cortex, followed by the frontal and cingulate cortices. These tau lesions were composed of 4-repeat tau. These

results were consistent with atypical PSP, which was diagnosed as PSP-FTD.

In vivo–in vitro correlation analyses

Biochemical analysis revealed the presence of 4-repeat tau in both cases. In subject 1, sarkosyl-insoluble tau was high in the parahippocampal gyrus and hippocampus, moderate in the globus pallidus and putamen, and low in other areas. The parahippocampal gyrus contained 3- and 4-repeat tau, suggesting that they are age-related tau. AT8 immunohistochemistry was positive in the brain sections from the same tissue. In subject 1, in vivo [^{18}F]THK-5351 binding was correlated significantly with sarkosyl-insoluble tau levels determined by Western blot analysis ($r = 0.67$, $P = 0.039$). In addition, we found strong correlations between in vivo [^{18}F]THK-5351 binding and MAO-B levels ($r = 0.78$, $P = 0.0096$), between in vivo [^{18}F]THK-5351 binding and GFAP level ($r = 0.67$, $P = 0.039$). In vitro [^{3}H]THK-5351 binding assay using brain homogenates also demonstrated a strong correlation between in vivo [^{18}F]THK-5351 retention and in vitro tracer binding in subject 1 ($r = 0.92$, $P = 0.005$). Tau and GFAP immunoreactivities in the brain sections were measured quantitatively for correlation analysis between in vivo tracer retention and histopathology. We observed positive correlation trends between in vivo [^{18}F]THK-5351 retention and tau loads ($r = 0.48$, $P = 0.06$), and between in vivo [^{18}F]THK-5351 retention and GFAP immunoreactivity ($r = 0.49$, $P = 0.05$). In subject 2, in vivo [^{18}F]THK-5351 binding was correlated significantly with tau-immunohistochemistry using AT8 antibody ($r = 0.48$, $P = 0.037$). Furthermore, in vivo [^{18}F]THK-5351 retention was correlated positively with the density of GFAP immunoreactive astrocytes ($r = 0.64$, $P = 0.0033$).

In vitro autoradiography

In vitro autoradiography of [^{18}F]THK-5351 in frozen sections demonstrated high tracer binding in the globus pallidus as well as putamen in subject 1 and in the frontal cortex in subject 2, which was consistent with in vivo PET results. These bindings were displaced completely after treatment with MAO-B inhibitor, Lazabemide. The spatial pattern of [^{18}F]THK-5351 binding was similar to that of MAO-B immunostaining, suggesting that the target of [^{18}F]THK-5351 binding was MAO-B positive astrogliosis rather than the tau aggregates in the PSP brain.

Discussion

Tremendous efforts have been made to develop tau-selective PET radiopharmaceuticals. The first-generation tau PET tracers, such as [^{11}C]PBB3, [^{18}F]AV1451, and [^{18}F]THK-5351, showed nonnegligible off-target binding. In this study, we expanded the imaging-pathology correlation analysis to autopsy-confirmed PSP cases showing two different clinical phenotypes, Richardson syndrome (PSP-RS) and PNFA.

A patient with PSP-RS showed the spatial distribution of [^{18}F]THK-5351 retention which was similar to cases of classic PSP-RS. Postmortem examination of this patient confirmed the existence of 4-repeat tau aggregates in these regions. However, imaging-pathology correlation analysis indicated a significant correlation between in vivo [^{18}F]THK-5351 retention and MAO-B level. Furthermore, in vitro autoradiography demonstrated that [^{18}F]THK-5351 binding in the globus pallidus was displaced by the MAO-B inhibitor, suggesting that [^{18}F]THK-5351 mainly binds to the MAO-B rather than the 4-repeat tau aggregates. In our previous study using paraffin-embedded fixed brain sections, we observed specific binding of [^{18}F]THK-5351 to tufted astrocytes and neurofibrillary tangles in the PSP brain[2)]. However, the fixation of tissues and use of alcohol in the differentiation process may affect the tracer binding in in vitro autoradiography experiments. In this study, we performed in vitro autoradiographs of fresh-frozen sections without using alcohol and found a substantial amount of tracer binding to MAO-B. Fresh-frozen section results showed good agreement with antemortem [^{18}F]THK-5351 PET analysis. These results highlighted the importance of appropriate experimental procedures in the validation of PET radiopharmaceuticals.

We observed a significant correlation between tau pathology and GFAP in both of our subjects. A postmortem study reported that the density of GFAP correlated with that of neurofibrillary tangles, but not with tufted astrocytes in PSP, suggesting the greater contribution of neurofibrillary tangles to astrogliosis in PSP[7)]. MAO-B is expressed dominantly in the mitochondrial outer membrane of astrocytes. Since elevation of MAO-B levels in the brain has been implicated in several neurodegenerative diseases, MAO-B is an attractive target as a molecular imaging marker of astrogliosis. Our study strongly supported that [^{18}F]THK-5351 PET dominantly reflected the binding to MAO-B in patients with PSP. Therefore, [^{18}F]THK-5351 PET would be useful for in vivo assessment of astrogliosis in PSP. Future research should proceed with development of PET tracers for selective detection of astrogliosis and sensitive detection of 4-repeat tau in the human brain.

References

1. Harada R, Okamura N, Furumoto S, et al., J Nucl Med 57(2016) 208.
2. Ishiki A, Harada R, Okamura N, et al. Eur J Neurol 24(2017) 130.
3. Kikuchi A, Okamura N, Hasegawa T, et al., Neurology 87(2016) 2309.
4. Ng KP, Pascoal TA, Mathotaarachchi S, et al., Alzheimers Res Ther 9(2017) 25
5. Harada R, Ishiki A, Kai H, et al., J Nucl Med 59(2017) 671
6. Ishiki A, Harada R, Kai H, et al., Acta Neuropathol Commun. 6(2018) 53
7. Togo T, Dickson DW. Acta Neuropathol 104(2012) 398

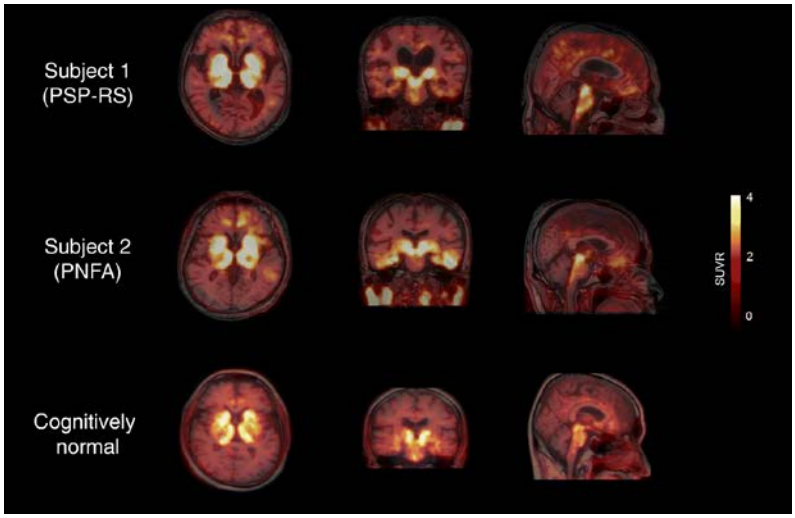

Figure 1. [^{18}F]THK-5351 PET images from two study subjects and a cognitively normal subject.